catalysts

MDPI

Article

Determination of Chemical Kinetic Parameters for Adsorption and Desorption of NH_3 in Cu-Zeolite Used as a $DeNO_x$ SCR Catalyst of Diesel Engines

Yanghwa Kim [1], Ocktaeck Lim [2] and Hongsuk Kim [3,*]

[1] Graduate School of Mechanical Engineering, University of Ulsan, Ulsan 44610, Korea
[2] School of Mechanical Engineering, University of Ulsan, Ulsan 44610, Korea
[3] Korea Institute of Machinery & Materials, Daejeon 34103, Korea
* Correspondence: hongsuk@kimm.re.kr; Tel.: +82-042-868-7367

Abstract: Ammonia-based selective catalytic reduction is one of the most effective NO_x reduction technologies for diesel engines, but its low NO_x reduction efficiency under low-temperature conditions needs further improvement. Previous studies have broadened our understanding of the NH_3 adsorption and desorption that occurs in an SCR catalyst of Cu ion-exchanged zeolite. However, many studies conducted to data on the control of the NH_3 adsorption and desorption in SCR catalysts have considered a simple chemical reaction related to a single acid site. This study demonstrates a detailed process for determining the chemical kinetic parameters of the adsorption and desorption of NH_3 for different types of acid sites of a zeolite catalyst. The determined chemical kinetics parameters will be used for more effective control of the SCR system in future studies.

Keywords: selective catalytic reduction; NH_3 temperature-programmed desorption; Cu-SSZ-13; NH_3 adsorption; NH_3 desorption

Citation: Kim, Y.; Lim, O.; Kim, H. Determination of Chemical Kinetic Parameters for Adsorption and Desorption of NH_3 in Cu-Zeolite Used as a $DeNO_x$ SCR Catalyst of Diesel Engines. *Catalysts* **2022**, *12*, 917. https://doi.org/10.3390/catal12080917

Academic Editors: Małgorzata Rutkowska and Lucjan Chmielarz

Received: 13 July 2022
Accepted: 16 August 2022
Published: 19 August 2022

1. Introduction

NO_x is a major air pollutant emitted from diesel vehicles. To reduce NO_x, selective catalyst reduction (SCR) systems have been widely used. Catalysts include large and medium pore zeolites such as ZSM-5, MOR, FER, and BEA, and small pore zeolites such as SSZ-13 and SAPO-34 [1]. Among the NH_3-SCR catalysts, small pore zeolite catalysts such as Cu-SSZ-13 and Cu-SAPO-34 are being actively studied for their excellent NO_x reduction efficiency and good hydrothermal stability [2–4]. Cu zeolite has a better SCR performance at low temperatures than Fe zeolite. Cu/SSZ-13 and Cu/SAPO are catalysts suitable for a wide temperature range with excellent hydrothermal stability, operating even below 350 °C [1].

Figure 1 shows the various forms of adsorbed NH_3 on Cu-zeolite, which was proposed by Chen et al. [5]. Figure 1a shows the NH_3 molecules bonded to the Brønsted acid site (BAS) in the form of NH_4^+, and Figure 1b–f represents NH_3 complexes bonded to Cu ions. The bonding form of Cu ions and NH_3 molecules varies depending on the degree of Cu ionization, the presence of OH- ions, and the number of adsorbed NH_3 molecules. NH_3 combined with Cu ions has a different SCR reaction pathway depending on the oxidation state of Cu. [6]. The NH_3 bound to the Cu^{2+} ion reacts with NO directly to form N_2 and H_2O via an NO-assisted NH_3 activation pathway, and the NH_3 bound to the Cu^{2+} ion is converted to Cu^+-H^+ in this process. Also, the Cu^+-H^+ oxidizes to Cu^{2+} with a reaction with O_2 and NO_2. In addition, the NH_3 bound to the Cu ion reacts with NO directly via an NO-assisted NH_3 activation pathway. On the other hand, the NH_3 bound to the Brønsted acid site is much less active under low-temperature steady-state conditions [7]. As such, it is important to understand the binding behavior of NH_3, because the mechanism of the SCR reaction varies depending on the binding state of NH_3.

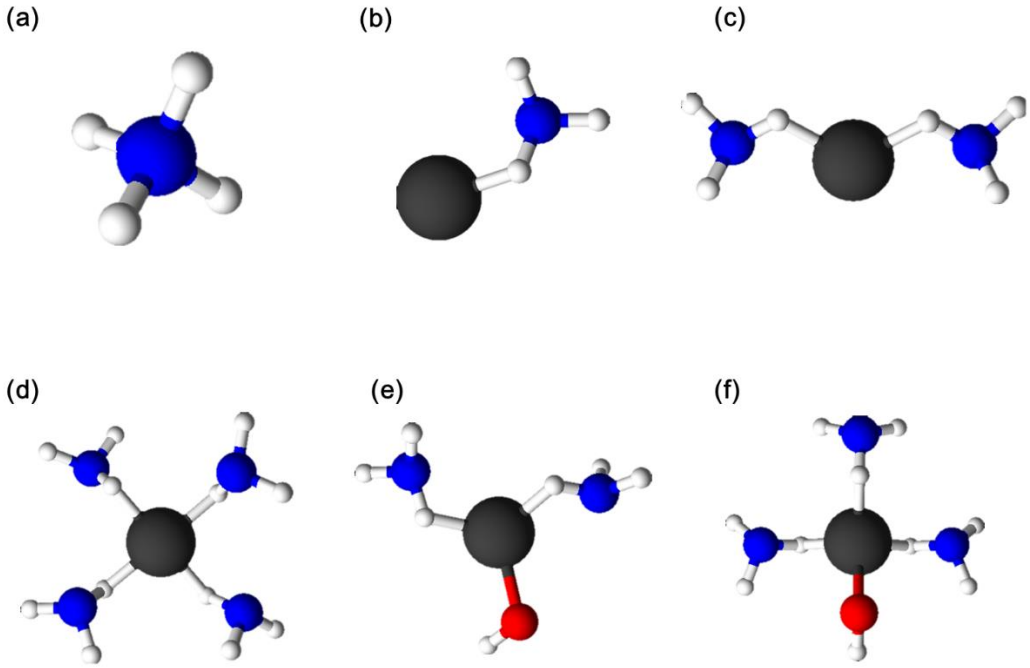

Figure 1. Atomic configurations of NH_3 complexes adsorbed in Cu-SSZ-13 zeolite as NH_3 molecules. (**a**) NH_4^+, (**b**) $[Cu(I)NH_3]^+$, (**c**) linear $[Cu(I)(NH_3)_2]^+$, (**d**) fourfold $[Cu(II)(NH_3)_4]^{2+}$, (**e**) $[Cu(II)(OH)(NH_3)_2]^+$, and (**f**) $[Cu(II)(OH)(NH_3)_3]^+$. Atom color codes: copper (gray), nitrogen (blue), oxygen (red), and hydrogen (white) [5].

The adsorption and desorption of NH_3 in an SCR catalyst are important phenomena which affect the SCR reaction. Many studies have investigated NH_3 adsorption and desorption by using various measuring techniques, such as NH_3 temperature-programmed desorption (TPD) and infrared (IR) spectroscopy [8–10]. Recent studies [5,6,11] have shown that there are many peaks of NH_3 desorption for Cu-zeolite catalysts according to the temperature range at which NH_3 is desorbed. Lezcano-Gonzalez et al. [10] observed two NH_3 desorption peaks in H-SSZ-13 and explained their chemical bonding structures. The first peak, called the low-temperature (LT) peak, is a desorption peak at approximately 180 °C. They explained that NH_3 molecules desorbed in the LT peak were weakly bound to the Lewis acid site (LAS) or solvated to NH_4^+ ions. The second peak is called the high-temperature (HT) peak, and occurs in the temperature range of approximately 450 °C. It was explained as NH_3 that is strongly bound to the BAS. Lezcano-Gonzalez et al. [11] compared the NH_3-TPD profiles of H-SSZ-13 and Cu-SSZ-13 and confirmed the absence of an intermediate temperature (IT) peak in H-SSZ-13. Further, when the amount of Cu ion exchange increased, the size of the IT peak increased, while that of the HT peak decreased. This indicates that the Cu ions in the catalyst affect the IT peak.

Chen et al. [5] explained these peaks by simulating the NH_3-TPD profile of Cu-CHA zeolite using discrete Fourier transform (DFT) calculations. They explained that the LT peak represents the desorption of NH_3 from LAS, along with NH_3 desorption from a $[Cu(II)(OH)(NH_3)_3]^+$ complex. The IT peak shown at 250–350 °C was attributed to the decomposition of a linear $[Cu(I)(NH_3)_2]^+$ complex and residual $[Cu(II)(OH)(NH_3)_3]^+$. The HT peak at 400–500 °C was attributed to NH_3 in the form of NH_4^+ adsorbed to the BAS, $[Cu(I)(NH_3)]^+$, and $[Cu(II)(NH_3)_4]^{2+}$.

Table 1 compares the NH_3 bonding mechanisms represented by the studies of Chen et al. [5] and Lezcano-Gonzalez et al. [11]. Chen et al. [5] suggested a more detailed bonding mechanism between Cu ions and NH_3 molecules. In contrast, Lezcano-Gonzalez et al. mentioned NH_3 molecules solvating NH_4^+ ions as a cause of the LT peak, and the extra-framework aluminum (EFAL) as a cause of another HT peak, which was not mentioned by Chen et al.

Table 1. NH_3 adsorption form organizing the NH_3 adsorption peak by temperature, as mentioned in various literature and papers.

Classification of NH_3 Desorption Peak	Study of Chen et al. [5]	Study of Lezcano-Gonzalez et al. [11]
Low-Temperature peak	LAS	LAS
	$[Cu(II)(OH)(NH_3)_3]^+$	NH_3 molecules solvating NH_4^+ ions
Intermediate-Temperature peak	$[Cu(I)(NH_3)_2]^+$	NH_3 adsorbed at the Cu^{2+} sites
	remained $[Cu(II)(OH)(NH_3)_3]^+$	
High-Temperature peak	NH_4^+ (BAS)	NH_4^+ (BAS)
	$[Cu(I)(NH_3)]^+$	EFAL (extra framework aluminum)
	$[Cu(II)(NH_3)_4]^{2+}$	

Yoshihisa et al. [5] compared the NH_3 adsorption and desorption of H-ZSM-5 and Cu-ZSM-5. Similarly to the study by Lezcano-Gonzalez et al. [11], Yoshihisa et al. observed that H-ZSM-5 had two NH_3 peaks in the LT and HT regions, while Cu-ZSM-5 had an additional peak in the IT region. Additionally, they found that the NO reduction reaction did not occur in the absence of Cu ions in the zeolite. This means that the Cu ion sites are very important for the SCR reaction, and the adsorption and desorption with various forms of NH_3 at the Cu sites should be comprehensively studied.

Gao et al. [12,13] and Paolucci et al. [14] demonstrated the importance of Cu-NH_3 intermediates, such as $[Cu(II)(OH)(NH_3)_3]^+$ and $[Cu(I)(NH_3)_2]^+$, in the low-temperature SCR reaction. As a starting point for the SCR reaction, they suggested that $[Cu(II)(OH)]^+$ adsorbs two NH_3 molecules and forms a complex of $[Cu(II)(OH)(NH_3)_3]^+$. When an NO molecule is introduced, the $[Cu(II)(OH)(NH_3)_3]^+$ changes to intermediates of NH_2-Cu(I)-NO or NH_3-Cu(I)-HONO by rearranging the NH_3 and NO ligands. Eventually, N_2 and H_2O are formed from these intermediates. Then, after the adsorption of another NH_3 molecule onto the Cu ion, $[Cu(I)(NH_3)_2]^+$ is formed. Next, two $[Cu(I)(NH_3)_2]^+$ intermediates and oxygen molecules combine to form $[Cu(I)(NH_3)_2]^+$-O_2-$[Cu(I)(NH_3)_2]^+$. The compound changes again to $[Cu(II)(OH)(NH_3)_3]^+$ via electron transfer from Cu to O and hydration with H_2O molecules. This means that the adsorption of ammonia to the Cu ion plays an important role in the NO-SCR cycle.

According to previous studies [15,16], NO_x removal efficiency at low temperatures can be improved by increasing the amount of NH_3 adsorption in the SCR catalyst. It is well known that NH_3 slip can be prevented by careful control of NH_3 adsorption and desorption at high temperatures. However, much of the previous research regarding NH_3 adsorption control for SCR systems of diesel engines considered the catalyst as a single acid site, even though the adsorption of NH_3 in zeolite is influenced by multiple acid sites with different characteristics. As far as we know, there has been no research showing a detailed experimental process to determine the chemical kinetic parameters of adsorption and desorption of NH_3 for different types of acid sites of a zeolite catalyst.

This study investigated the adsorption and desorption of NH_3 on various kinds of acid sites of Cu-SSZ-13 zeolite and attempted to determine their chemical kinetic parameters, which are needed for more precise control of the SCR reaction.

2. Results and Discussion

In the SCR reaction modeling, information on both the NH_3 adsorption rate and desorption rate are necessary. In the single-site model, the NH_3 adsorption rate, r_{ads}, can be expressed using Equation (1):

$$r_{ads} = k_{ads} C_{NH_3} (1 - \theta_{NH_3}) \quad (1)$$

where k_{ads} is the reaction constant and C_{NH_3} is the mole concentration of NH_3. θ_{NH_3} is the surface coverage of the catalyst by NH_3 molecules. It is defined as:

$$\theta_{NH_3} = \frac{N_{NH_3}}{N*_{NH_3}} \quad (2)$$

where N_{NH_3} is the amount of NH_3 molecules adsorbed on the catalyst and $N*_{NH_3}$ is the maximum amount of NH_3 molecules adsorbed on the catalyst.

The NH_3 desorption rate, r_{des}, of the single-site model is generally expressed as follows:

$$r_{des} = k_{des} \cdot \exp\left(-\frac{E_{des}}{RT}\right)\theta_{NH_3} \quad (3)$$

where k_{des} is the reaction constant and C_{NH_3} is the mole concentration of NH_3. E_{des} is the activation energy. R and T are the universal gas constant and catalyst temperature, respectively.

In this study, we attempted to extend the above single-site model to a multi-site model to provide more detailed information on NH_3 adsorption and desorption rates. In the next section, the modified forms of Equations (2) and (3) are shown for the multi-site model.

In this study, only the chemically adsorbed NH_3 molecules were considered. Figure 2a shows that the amount of physically adsorbed NH_3 molecules increased as the NH_3 supply time increased. At the beginning of the NH_3 gas supply, the chemical bonds on the acid sites are superior. Therefore, the physical adsorption rate of NH_3 gas molecules is small. After that, the physical adsorption rate increases, because the number of acid sites available for chemical bonding is decreased. In addition, when a large amount of ammonia molecules are physically adsorbed, the physical adsorption rate decreases again due to the limitation of molecular diffusion. The experimental results also showed that the physical adsorption rate is small at the beginning, then increases rapidly, and decreases at the end. When the ammonia supply in the feed gas is stopped, the physically adsorbed ammonia is desorbed into the feed gas due to the difference between the ammonia concentration in the feed gas and the ammonia concentration on the catalyst surface. Figure 2b show the effect of temperature on the physically adsorbed NH_3 molecules. It decreases as the NH_3 supply temperature increases. This is because the attraction surface force, which acts between the catalyst surface and ammonia molecules, becomes smaller than the kinetic energy of the ammonia molecules, which is increased when the feed gas temperature increases. S. J. PALMER [17] presented a mathematical relationship showing that the surface force of water becomes smaller with an increase in temperature, which proves the validity of the results obtained in Figure 2.

Figure 3 shows the variation of NH_3-TPD curves with the NH_3 supply time. The 7500 s curve consisted of three peaks. Many researchers have found the same results from similar experiments. These three peaks have been called the LT peak (~200 °C), IT peak (200–400 °C), and HT peak (~400 °C). The curves below 937 s show that NH_3 was mainly desorbed at the HT peak of 400 °C or more. This indicates that the initial adsorption of NH_3 molecules occurred in the acid sites of the HT peak, which had a high bonding energy. When the NH_3 supply time was increased to 1406 s, the HT peak grew and the smaller IT peak appeared. Further, when the NH_3 supply time was increased to 1875 s, the LT peak appeared at temperatures below 200 °C. According to studies by several researchers, the HT peak was mainly related to the NH_3 molecules, which are strongly bonded to BAS, and the IT peak was related to the NH_3 molecules that were adsorbed to Cu ions. Additionally, it seems that the LT peak comprised weakly bonded NH_3 molecules in the form of $[Cu(II)(OH)(NH_3)_3]^+$ or solvated to NH_4^+ ions.

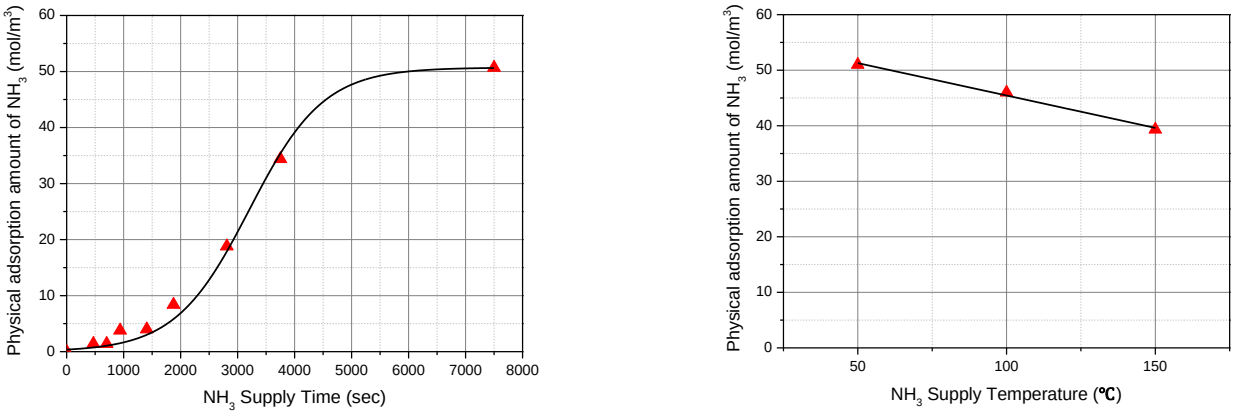

(**a**) (**b**)

Figure 2. Variation of the physically adsorbed NH_3 amount according to the various parameters: (**a**) Effect of NH_3 supply time (inlet NH_3 concentration: 200 ppm, temperature of NH_3 absorption: 50 °C); (**b**) effect of NH_3 adsorption temperature (inlet NH_3 concentration: 200 ppm, NH_3 supply time: 7500 s).

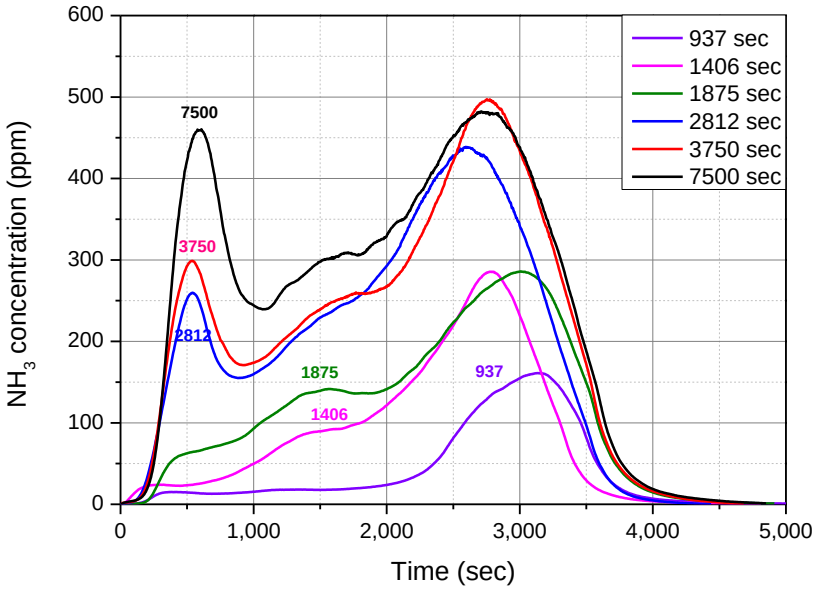

Figure 3. Variation of NH_3-TPD curves with respect to the NH_3 supply time (inlet NH_3 concentration: 200 ppm, temperature of NH_3 absorbing: 50 °C).

Figure 4 shows the results of NH_3 TPD tests obtained at different NH_3 adsorption temperatures of 50 °C, 100 °C, and 150 °C. In the three experiments, 200 ppm of NH_3 gas was supplied to the catalyst for 7500 s equally. Therefore, the same amount of NH_3 was supplied. According to the results of these experiments, the shapes of the HT peaks of the three different temperature conditions were nearly the same. However, the LT peak disappeared, and the IT peak increased as the NH_3 adsorption temperature increased from 50 °C to 100 °C and then to 150 °C. The large size of the LT peak and the small size of the IT peak at 50 °C indicate that the LT peak interrupts the growth of the IT peak. This means that the LT peak and IT peak are chemically related. As suggested by Chen et al. [5], the OH of $[Cu(II)(OH)(NH_3)_3]^+$ in the LT peak is separated at 100 °C or higher, and it is changed to $[Cu(I)(NH_3)_2]^+$ and moved to the IT peak.

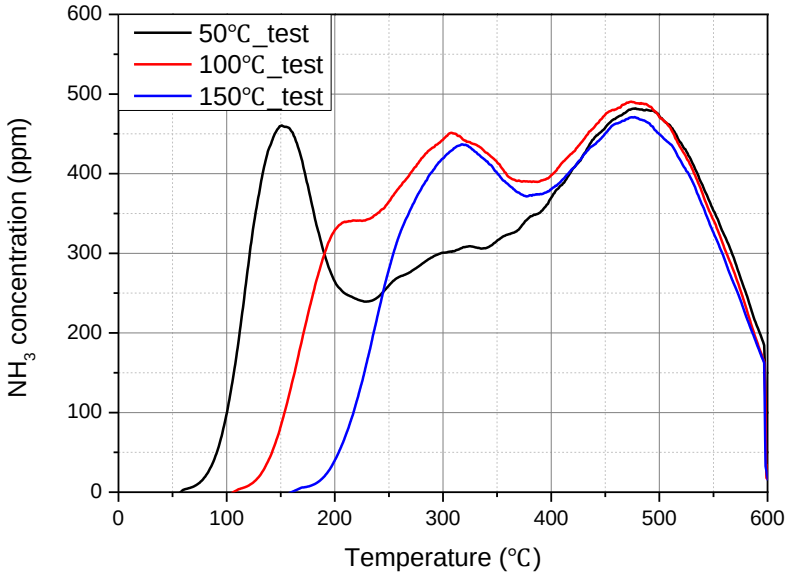

Figure 4. The effect of the NH_3 adsorption temperature on the NH_3-TPD test (NH_3 supply concentration: 200 ppm, NH_3 supply time: 7500 s).

Comparing the HT peaks of 2812 and 7500 s in Figure 5 and the HT peaks at 50 °C, 100 °C, and 150 °C in Figure 4, the height and width of the HT peaks are almost the same. This means that when the adsorption time is sufficiently long, the HT peak converges to a certain shape. Therefore, the number of acid sites for the HT peak is finite. Similarly, it seems that the shape of the IT peaks in Figures 3 and 4 eventually converged to that of the IT peak at 150 °C, as shown in Figure 4. To describe the degree of NH_3 adsorption at the acid sites, the term surface coverage (θ_{NH_3}) was used in this study. Coverage of the HT and IT peaks is defined in Equations (4) and (5), as follows:

$$\theta_{NH_3\_HT} = \frac{N_{HT}}{N*_{HT}} \quad (4)$$

$$\theta_{NH_3\_IT} = \frac{N_{IT}}{N*_{IT}} \quad (5)$$

where N_{HT} and N_{IT} are the amounts of NH_3 molecules adsorbed in the HT and IT peaks, respectively. $N*_{HT}$ and $N*_{IT}$ are the maximum catalyst adsorption capacities of the HT and LT peaks, respectively.

However, the size of the LT peak continued to increase and did not converge, as shown in Figures 3 and 4. This means that the rate of NH_3 adsorption of the LT peak was not expressed as a function of coverage.

Figure 5 shows an example of curve fitting for the NH_3 TPD test results. This study assumed that the LT, IT, and HT peaks of the TPD curve can be expressed using standard normal distribution curves. In this example, the difference between the total amount of NH_3 adsorption obtained by integrating the TPD curve and that obtained by integrating the three standard normal distribution curves was only 0.56%. Thus, it can be said that analysis using curve fitting did not cause a significant error. The integrated amount of NH_3 of the peaks presented in this paper were obtained from curve fitting with standard normal distribution curves.

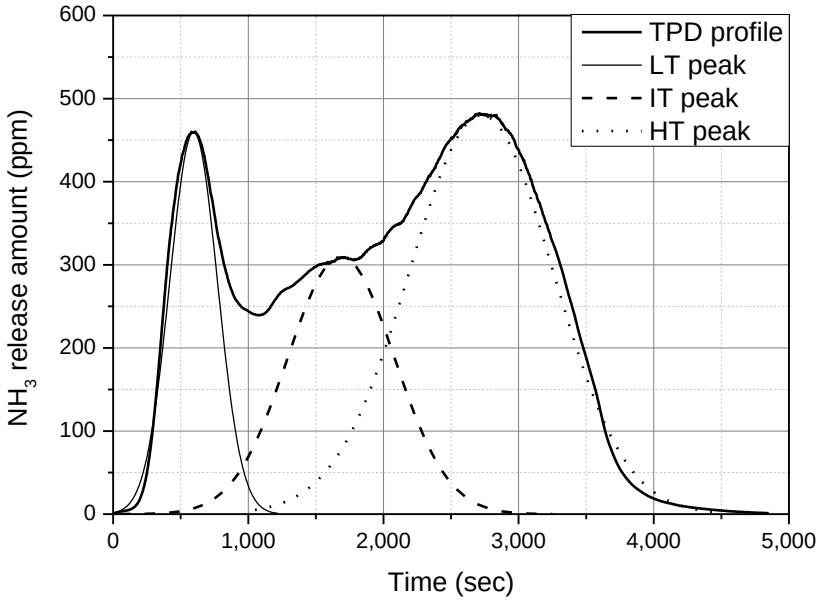

Figure 5. An example of curve fitting of TPD curve with three normal distribution curves of the LT, IT, and HT peak (inlet NH_3 concentration: 200 ppm, NH_3 supply time: 7500 s, temperature of NH_3 absorbing: 50 °C).

Figure 6 shows the change in the NH_3 adsorption amount of each peak with respect to time. It was obtained from the curves shown in Figure 5 by integrating the HT, IT, and LT peaks. The NH_3 adsorption amount of the HT and IT peaks increased rapidly at the beginning and then became saturated at a certain value. However, it seems that the saturation of the LT peak was not clear as the NH_3 supply time increased. Many other studies [11,18,19] have shown that solvation of the ammonium Ion (NH_4^+) by NH_3 can occur under low temperatures. This solvation is independent to acid sites, and quite a large amount of NH_3 molecules attach as a form of $NH_4^+ \cdot (NH_3)_n$. Here, n is the number of NH_3 molecules attached to ammonium ions. Because of this, linear curve fitting was used to describe the development of NH_3 adsorption amount of the LT peak. Additionally, we found that the total amount of NH_3 adsorption of the HT peak was the largest, that of the IT peak was second, and that of the LT peak was the smallest.

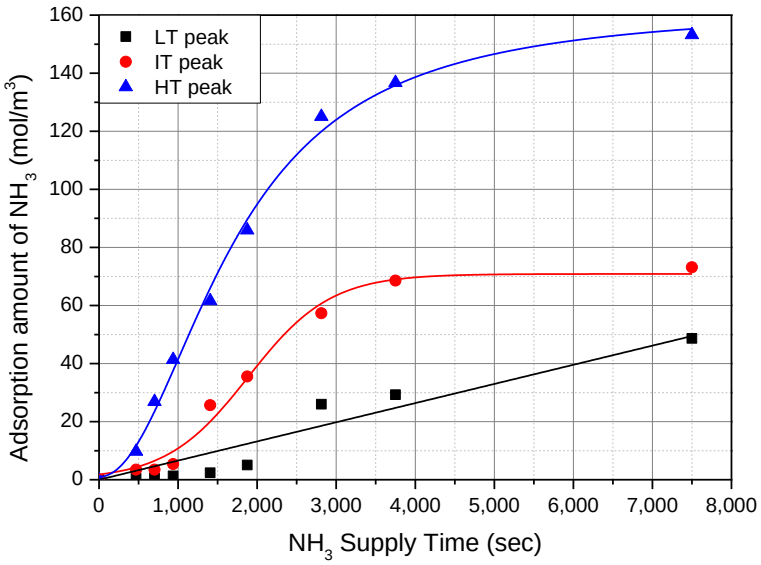

Figure 6. Change in the amount of NH_3 adsorption of each peak with respect to NH_3 supply time (inlet NH_3 concentration: 200 ppm, temperature of NH_3 absorbing: 50 °C).

Figure 7 shows the re-plotted graph of Figure 6 with the relationship between θ and the NH_3 supply time. For the calculation of θ, the values of Ω^*_{HT} of 153 mol/m^3 and Ω^*_{IT} of 99 mol/m^3 were used, respectively. These values were obtained from the integration of the saturated HT and IT peaks shown in Figures 3 and 4, respectively. As already mentioned, the LT peak continued to grow and did not converge to a specific shape, so the NH_3 adsorption rate cannot be expressed as a function of θ, and it is not included in Figure 7.

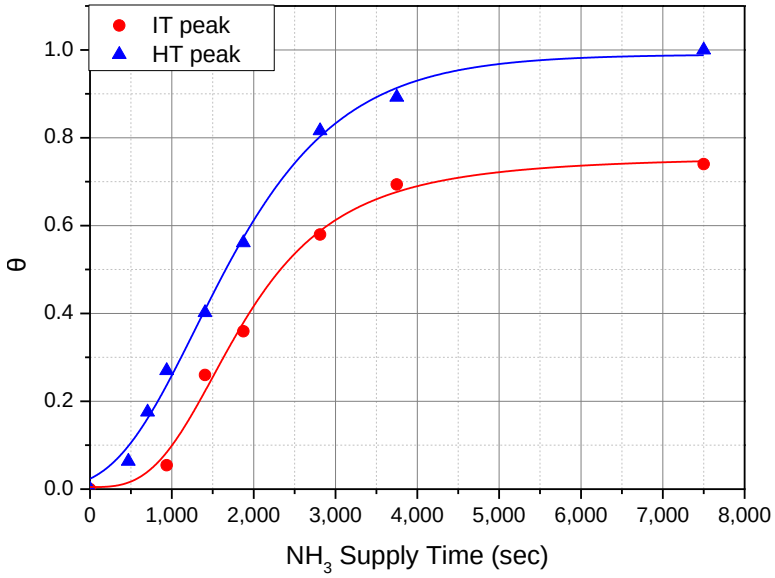

Figure 7. Change in θ of the HT and IT peaks according to NH_3 supply time (inlet NH_3 concentration: 200 ppm, temperature of NH_3 absorbing: 50 °C).

Figure 8 shows the correlation between $d\theta_{HT}/dt$ and $(1-\theta_{HT})$ for NH_3 adsorption, which was replotted with the data of Figure 7. It seems that $d\theta_{HT}/dt$ is proportional to $(1-\theta_{HT})$. This means that the reaction rate of adsorption of NH_3 molecules on the acid sites constituting the HT peak can be expressed by the first-order equation for $(1-\theta_{HT})$. The reason for some deviations from the linear relationship seem to be due to factors that were not managed precisely during the experiment, such as different external conditions (moisture and temperature) and changes in the catalyst state that occurred during the experiment.

Figure 9 shows the correlation between $d\theta_{IT}/dt$ and $(1-\theta_{IT})$ for NH_3 adsorption. Unlike the HT peak in Figure 8, a very small value of $d\theta_{IT}/dt$ was observed at the initial stage of NH_3 adsorption. Subsequently, $d\theta_{IT}/dt$ had a maximum value at θ of ~0.2, and thereafter, it tended to decrease as θ_{IT} increased. The NH_3 molecules were first adsorbed to the strong acid sites of the HT peak, and then the acid sites of the IT peak were filled with NH_3 molecules. This led to a low NH_3 adsorption rate for the IT peak at the initial stage of NH_3 adsorption. However, in the absence of the influence of the acid sites of the HT peak, the rate of adsorption of ammonia to the acid sites of IT peak seems to be linearly proportional to $(1-\theta_{IT})$. The deviations from the linear relationship in Figure 9 mean that the rate of NH_3 adsorption to acid sites in the IT peak was not only affected by $(1-\theta_{IT})$, but also other factors. Additionally, it can be said that these deviations were larger than in Figure 8. This means that the rate of NH_3 adsorption to acid sites of the IT peak is affected by more factors than the HT peak. In addition to the external air temperature, humidity, and catalyst state described in Figure 8, the influence of acid sites of the HT peak and LT peak are alsoincluded in these factors.

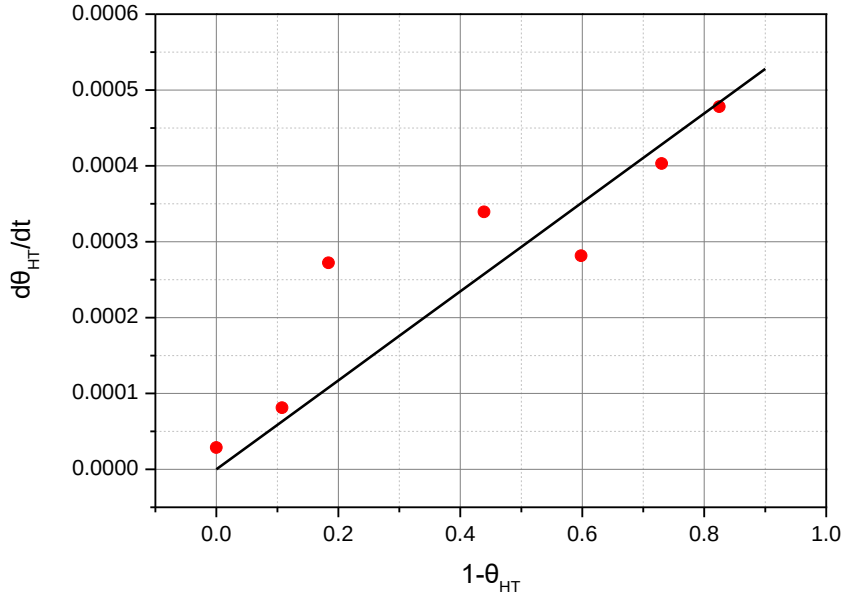

Figure 8. The relationship of $d\theta_{HT}/dt$ and $1-\theta_{HT}$ (inlet NH_3 concentration: 200 ppm, temperature of NH_3 absorbing: 50 °C).

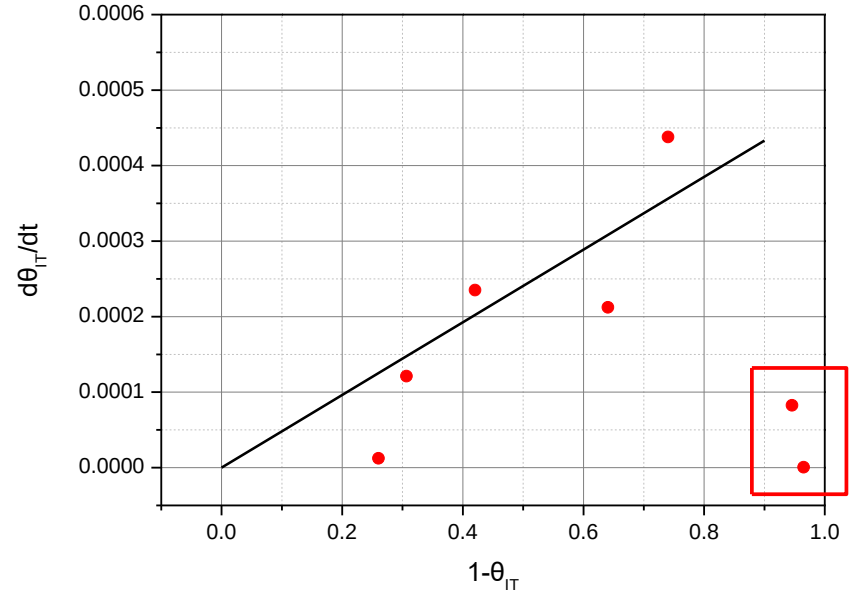

Figure 9. The relationship of $d\theta_{IT}/dt$ and $(1-\theta_{IT})$ (inlet NH_3 concentration: 200 ppm, temperature of NH_3 absorbing: 50 °C).

To date, many researchers have attempted to calculate the rate of NH_3 adsorption and desorption of a zeolite catalyst as a single-site model. Although the single-site model has the advantage of being simple, it is limited in providing an effective description of the phenomena of NH_3 adsorption and desorption.

This study suggests the modification of Equation (3) to describe the NH_3 adsorption rates as Equation (6) for the acid sites in the HT peak, and Equation (7) for the acid sites in the IT peak.

$$r_{ads\_HT} = k_{ads\_HT} C_{NH_3} (1 - \theta_{HT}) \quad (6)$$

$$r_{ads\_IT} = k_{ads\_IT} C_{NH_3} (1 - \theta_{IT}) \quad (7)$$

The values of k_{ads_HT} and k_{ads_IT} can be determined from the slopes of Figures 8 and 9, respectively.

To effectively describe the desorption phenomenon of ammonia molecules on the Cu SSZ-13 zeolite catalyst, it is desirable to express the desorption rates of the IT peak and HT peak separately. The NH_3 desorption rate can be described as follows:

$$r_{des\_HT} = k_{des\_HT} * \exp\left(-\frac{E_{des\_HT}}{RT}\right)\theta_{NH_3\_HT} \quad (8)$$

$$r_{des\_IT} = k_{des\_IT} * \exp\left(-\frac{E_{des\_IT}}{RT}\right)\theta_{NH_3\_IT} \quad (9)$$

Figures 10 and 11 introduce the process to find k_{des_HT}, k_{des_IT}, E_{des_HT}, and E_{des_IT} in Equations (8) and (9).

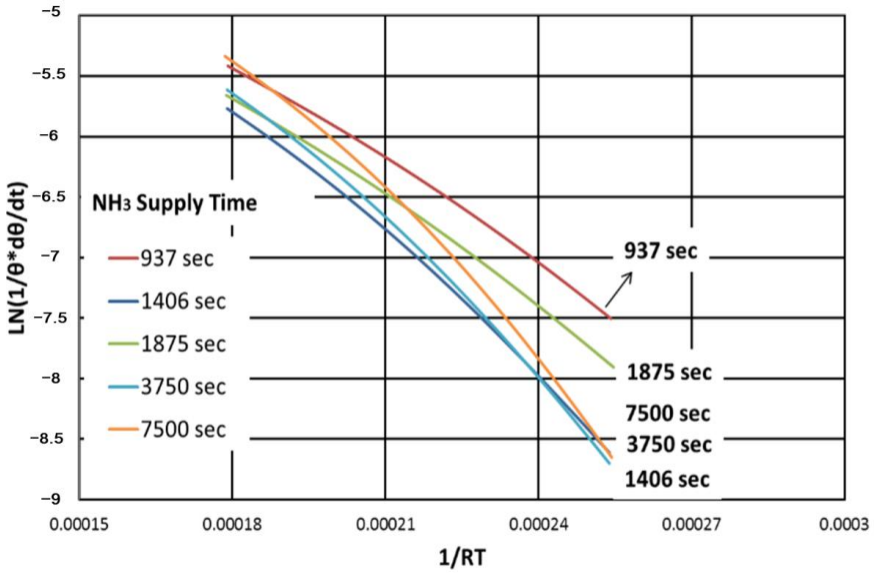

Figure 10. The relationship of the NH_3 desorption rate and temperature for the IT peak.

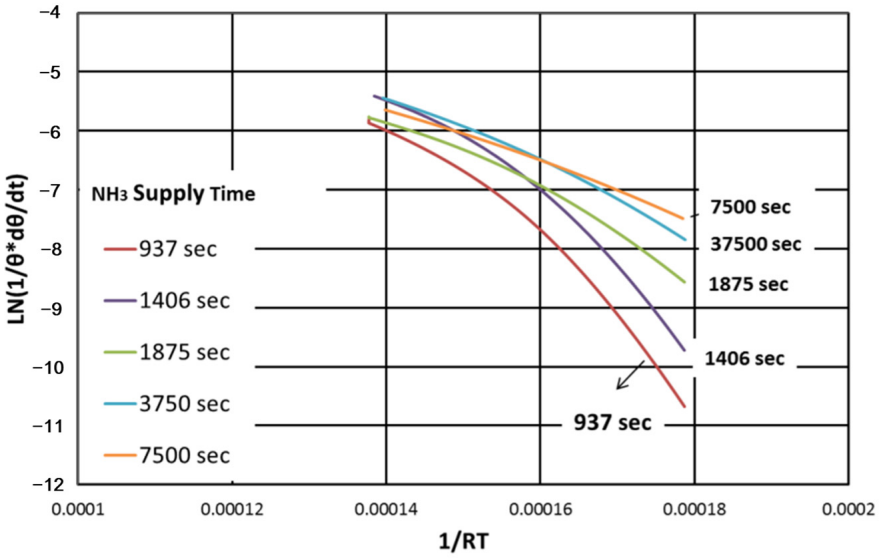

Figure 11. The relationship of the NH_3 desorption rate and temperature for the HT peak.

Figure 10 shows the relationship between ln(1/θ*dθ/dt) and 1/(RT) of the IT peak. In this graph, the slope represents the value of the activation energy of the reaction, and the log value of the *y*-axis intercept indicates the Arrhenius reaction constant. A nearly linear relationship between ln(1/θ*dθ/dt) and 1/(RT) is shown at each curve. However, the slopes and the values of *y*-axis intercept of each curve show some deviations, with no clear trend. The reason for this deviation is uncertain. The deviations may be caused by the experimental method, or by ambient conditions.

Figure 11 shows the NH_3 desorption rate of the HT peak as a function of ln(1/θ*dθ/dt) versus 1/(RT). The slope of the curve, which represents the activation energy, decreased when the NH_3 supply time was increased. This means that in the SSZ-13 catalyst, various acid sites with different degrees of acidity are widely distributed in the HT peak. These results show that NH_3 molecules adsorbed early in the reaction had stronger bonding and higher activation energy than NH_3 molecules adsorbed later.

From the above experimental results, we found that the activation energy and pre-exponential factor of the HT peak and LT peak gradually changed as the process of ammonia desorption proceeded. This study determined the averaged values of activation energy and the pre-exponential factor. It is necessary to find a more effective method to express the change of these values with time. However, the averaged kinetic parameters give the advantage of simple calculation.

Table 2 shows the values of the kinetic parameters for Equations (6)–(9), which were determined from the experimental results for NH_3 concentrations of 200 ppm. These values can be used effectively to describe the NH_3 adsorption and desorption of a zeolite catalyst.

Table 2. The values of k_{ads}, k_{des}, and E_{des} of the HT and IT peaks.

	k_{ads}		k_{des}		E_{des} (kJ/mol)	
peak	IT	HT	IT	HT	IT	HT
values	2.4×10^{-6}	2.9×10^{-6}	11.2	2.5×10^{5}	42.7	94.6

3. Experimental Equipment and Methods

3.1. Experimental Equipment

A schematic of the experimental setup is shown in Figure 12. It was composed of a gas feeding device, a catalyst, electric heaters to increase the temperature, and a gas analyzer. N_2, CO_2, and NH_3 gases were supplied, and their flow rates were controlled using mass flow controllers (MFC). The catalyst used in this study was Cu-SSZ-13 zeolite, which was commercialized by a motor company for EURO-6 heavy-duty diesel vehicles. The general properties of the Cu-SSZ-13 zeolite can be found in the reference from the manufacturer [20]. The catalyst was coated onto a honeycomb-type ceramic monolith. The diameter and length of the catalyst were 2 cm and 1 cm, respectively. The temperatures of the feeding gas and catalyst were controlled using electric heaters. The gases, including NH_3, were measured using FT-IR spectroscopy.

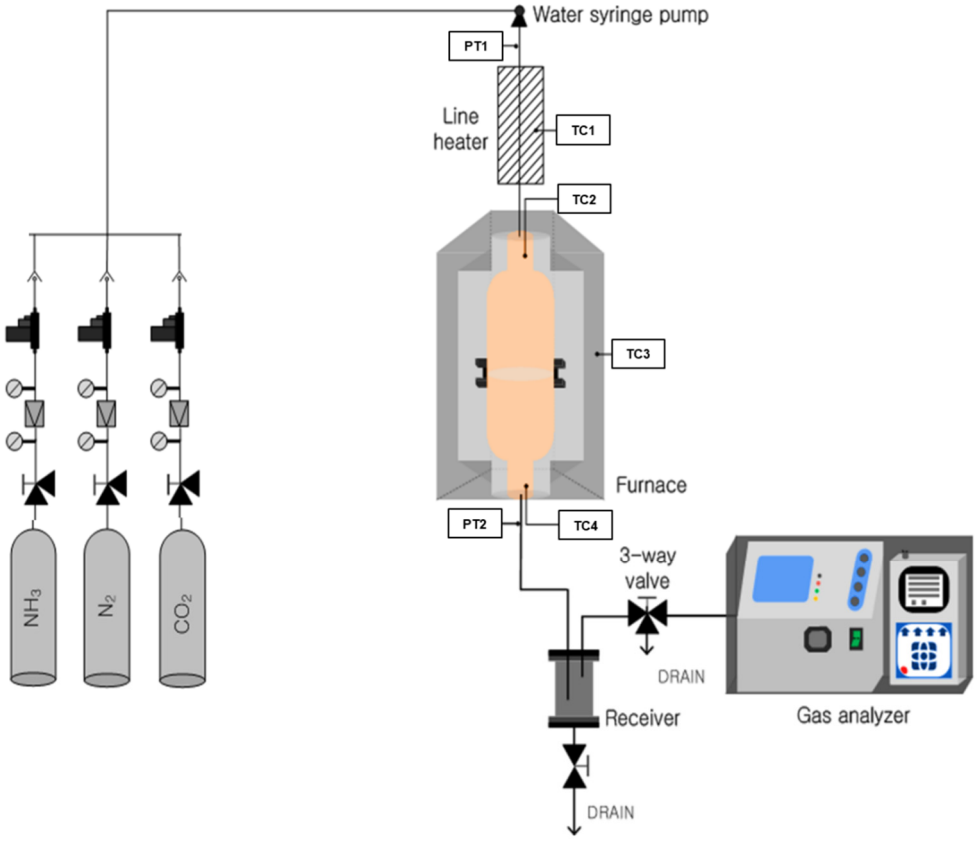

Figure 12. Schematic diagram of the experimental setup for the NH_3-TPD test.

3.2. Experimental Method

After adsorbing NH_3 to a catalyst at a low temperature, a temperature-programmed desorption (TPD) test was conducted. The experimental conditions are presented in Table 3. The NH_3 supply time, NH_3 concentration, and catalyst temperature during the NH_3 adsorption process were considered as the experimental parameters.

Table 3. Experimental conditions.

NH3 Adsorption Process	
NH3 concentration (ppm)	200
NH3 supply time (s)	469, 703, 1406, 1875, 2812, 3750, 7500
Catalyst temperature	50, 100, 150
Space velocity (/h)	40,000
NH3 Desorption Process	
Temperature range (°C)	50–600
Temperature rise time (°C/min)	9
N2 gas space velocity (/h)	20,000

Before adsorbing NH_3, N_2 gas was first supplied to the catalyst and the catalyst was heated to 600 °C to remove any existing impurities. After cooling the catalyst, N_2, CO_2, and NH_3 gases were supplied to adsorb NH_3 molecules while maintaining a certain temperature. After supplying a pre-determined amount of NH_3, the NH_3 supply was stopped, but N_2 and CO_2 were continuously supplied to remove physically adsorbed NH_3 molecules from the catalyst. After that, the catalyst was heated to 600 °C at a rate of 9 °C/min. During the heat-up process, the concentration of NH_3 desorbed from the catalyst

was measured using FT-IR (MKS, Andover, MA, USA). The results shown in this study were the averaged value of three repetitions of the test. The test set-up and procedure used in this study were similar to that already presented by Schiavoni et al. [21] and by Galloni et al. [22]. Figure 13 represents the above mentioned experimental procedure in more detail. It shows the change in the supply amount of various gases and temperature with time. One example of the concentration of NH_3 gas measured by FT-IR is also shown.

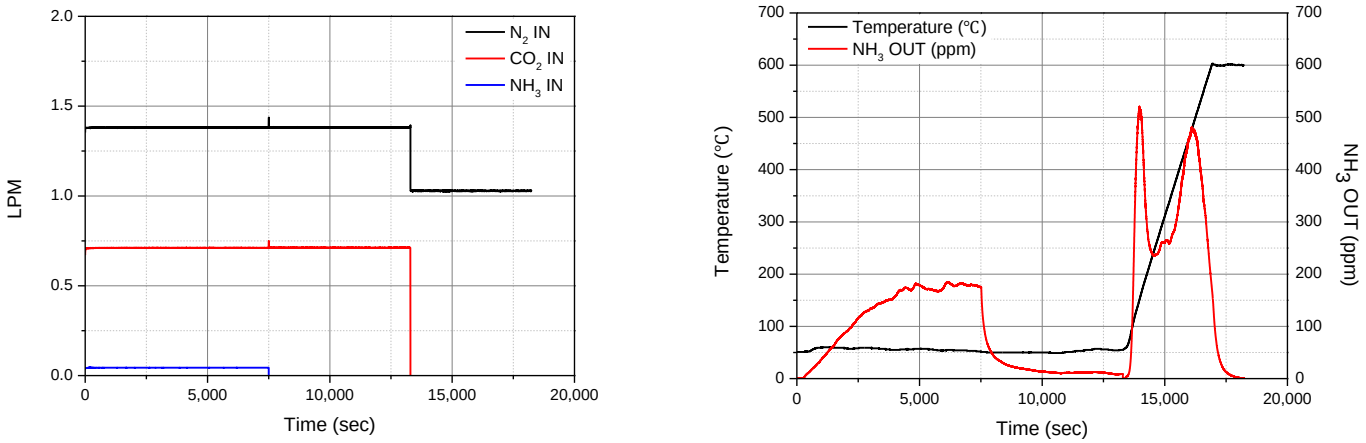

Figure 13. Changes in gas supply amount, temperature, and NH_3 concentration with time, describing the experimental procedure: (**a**) Gas-feeding amount; (**b**) temperature and NH_3 gas concentration.

4. Conclusions

NH_3 adsorption and desorption are important phenomena in NH_3-SCR of NO_x. Many studies which have tried to control the amount of NH_3 adsorption and desorption in zeolite catalyst have assumed that it has only one kind of acid site. This simple modeling has limitations, so this study aimed to develop equations of chemical kinetics describing the reaction rates of NH_3 adsorption and desorption in two important acid sites for NH_3-SCR. The following conclusions were obtained:

1. Physically adsorbed NH_3 molecules are weakly bound to the zeolite surface, not to the acid site, and do not appear to have a significant effect on the NO_x SCR reaction. Therefore, the effect of physically adsorbed NH_3 was excluded in this study.
2. The adsorption and desorption rates of the LT peak cannot be expressed with the NH_3 coverage ratio of the catalyst. The saturation of the LT peak cannot be confirmed because of solvation of ammonium ions by NH_3 molecules.
3. The adsorption rate of the HT peak can be expressed as a conventional linear function. The adsorption rates of the HT peak can be described as Equation (6).
4. However, it is not easy to express the rate of NH_3 adsorption of the IT peak because it is affected by the acid sites of the HT peak and interaction with NH_3 molecules of the LT peak. In this study, it was found that the rate of NH_3 adsorption of the IT peak can be expressed by Equation (7) when there is no influence of the acid sites of the HT peak and interaction with the NH_3 molecules of the LT peak.
5. The desorption rates of NH_3 molecules of the HT peak and IT peak can be described as Equations (8) and (9). The averaged chemical kinetics parameters describing NH_3 desorption rates for both the IT and HT peaks were determined.

Author Contributions: Conceptualization, Y.K. and H.K.; methodology, Y.K. and H.K.; validation, Y.K., O.L. and H.K.; formal analysis, H.K.; investigation, Y.K.; resources, O.L. and H.K.; data curation, Y.K.; writing—original draft preparation, Y.K.; writing—review and editing, H.K.; visualization, Y.K.;

supervision, H.K.; project administration, H.K.; funding acquisition, H.K. All authors have read and agreed to the published version of the manuscript.

Funding: This research was funded by the Korea Institute of Machinery & Materials, Republic of Korea, under the project name of "The ultra clean machinery technologies of future electric generation or power systems against PM2.5 fine particles and greenhouse gases" (Grant NO. NK237A). This research was also supported by the "Regional Innovation Strategy (RIS)" of the National Research Foundation of Korea (NRF) and the Ministry of Education (MOE) (2021RIS-003).

Data Availability Statement: Not applicable.

Conflicts of Interest: The authors declare no conflict of interest.

References

1. Mohan, S.; Dinesha, P.; Kumar, S. NOx reduction behaviour in copper zeolite catalysts for ammonia SCR systems: A review. *Chem. Eng. J.* **2020**, *384*, 123253. [CrossRef]
2. Beale, A.M.; Gao, F.; Lezcano-Gonzalez, I.; Peden, C.H.F.; Szanyi, J. Recent advances in automotive catalysis for NO_x emission control by small-pore microporous materials. *Chem. Soc. Rev.* **2015**, *44*, 7371–7405. [CrossRef] [PubMed]
3. Srivastava, R.K.; Neuffer, W.; Grano, D.; Khan, S.; Staudt, J.E.; Jozewicz, W. Controlling NOx emission from industrial sources. *Environ. Prog.* **2005**, *24*, 181–197. [CrossRef]
4. Colombo, M.; Koltsakis, G.; Nova, I.; Tronconi, E. Modelling the NH_3 adsorption-desorption process over an Fe-zeolite catalyst for SCR automotive applications. *Catal. Today* **2012**, *188*, 42–52. [CrossRef]
5. Chen, L.; Janssens, T.V.W.; Skoglundh, M.; Grönbeck, H. Interpretation of NH3-TPD Profiles from Cu-CHA Using First-Principles Calculations. *Top. Catal.* **2019**, *62*, 93–99. [CrossRef]
6. Tsukamoto, Y.; Utaki, S.; Fukuma, T.; Kusaka, J. Reactivity Analysis and Modeling of Cu-SCR Based on NH3-SCR Mechanism Considering Cu Redox. *Trans. Soc. Automot. Eng. Jpn.* **2018**, *49*, 1211–1216.
7. Zhang, Y.; Peng, Y.; Li, K.; Liu, S.; Chen, J.; Li, J.; Gao, F.; Peden, C.H.F. Using Transient FTIR Spectroscopy to Probe Active Sites and Reaction Intermediates for Selective Catalytic Reduction of NO on Cu/SSZ-13 Catalysts. *ACS Catal.* **2019**, *9*, 6137–6145. [CrossRef]
8. Niwa, M.; Katada, N. New Method for the Temperature-Programmed Desorption (TPD) of NH_3 Experiment for Characterization of Zeolite Acidity: A Review. *Chem. Rec.* **2013**, *13*, 432–455. [CrossRef] [PubMed]
9. Noda, T.; Suzuki, K.; Katada, N.; Niwa, M. Combined study of IRMS-TPD measurement and DFT calculation on Brønsted acidity and catalytic cracking activity of cation-exchanged Y zeolites. *J. Catal.* **2008**, *259*, 203–210. [CrossRef]
10. Rodríguez-Gonzalez, L.; Rodríguez-Castellon, E.; Jimenez-Lopez, A.; Simon, U. Correlation of TPD and impedance measurements on the desorption of NH_3 from zeolite H-ZSM-5. *Solid State Ionics* **2008**, *179*, 1968–1973. [CrossRef]
11. Lezcano-Gonzalez, I.; Deka, U.; Arstad, B.; Deyne, A.; Hemelsoet, K.; Waroquier, M.; van Speybroeck, V.; Weckhuysen, B.; Beale, A. Determining the storage, availability and reactivity of NH_3 within Cu-Chabazite-based NH_3 selective catalytic reduction systems. *Phys. Chem. Chem. Phys.* **2014**, *16*, 1639–1650. [CrossRef] [PubMed]
12. Gao, F.; Walter, E.D.; Kollar, M.; Wang, Y.; Szanyi, J.; Peden, C.H. Understanding NH_3 selective catalytic reduction kinetics over Cu/SSZ-13 from motion of the Cu ions Author links open overlay panel. *J. Catal.* **2014**, *319*, 1–14. [CrossRef]
13. Gao, F.; Mei, D.; Wang, Y.; Szanyi, J.; Peden, C.H.F. Selective Catalytic Reduction over Cu/SSZ-13: Linking Homo- and Heterogeneous Catalysis. *J. Am. Chem. Soc.* **2017**, *139*, 4935–4942. [CrossRef] [PubMed]
14. Paolucci, C.; Khurana, I.; Parekh, A.A.; Li, S.; Shih, A.J.; Li, H.; Di Iorio, J.R.; Albarracin-Caballero, J.D.; Yezerets, A.; Miller, J.T.; et al. Dynamic multinuclear sites formed by mobilized copper ions in NO_x selective catalytic reduction. *Science* **2017**, *357*, 898–903. [CrossRef] [PubMed]
15. Devarakonda, M.; Lee, J.; Muntean, G.; Pihl, J.; Daw, S. *1D Model of a Copper Exchanged Small Pore Zeolite Catalyst Based on Transient SCR Protocol*; SAE Technical Paper 2013-01-1578; SAE International: Warrendale, PA, USA, 2013. [CrossRef]
16. Lowell, S.; Shields, J.E. *Powder Surface Area and Porosity*; Particle Technology Series; Springer: Berlin/Heidelberg, Germany, 1991; Volume 2. [CrossRef]
17. Palmer, S.J. The effect of temperature on surface tension. *Phys. Educ.* **1976**, *11*, 119–120. [CrossRef]
18. Bonelli, B.; Armandi, M.; Areán, C.O.; Garrone, E. Ammonia-Solvated Ammonium Species in the NH4-ZSM-5 Zeolite. *ChemPhysChem* **2010**, *11*, 3255–3261. [CrossRef] [PubMed]
19. Payzant, J.D.; Cunningham, A.J.; Kebar, P. Gas Phase Solvation of the Ammonium Ion by NH, and HzO and Stabilities of Mixed Clusters NH4+(NH3),(HzO). *Can. J. Chem.* **1973**, *51*, 3242. [CrossRef]
20. BASF Corporation. Emissions Treatment System with Ammonia-Generating and SCR Catalysts. PCT/US2010/029329, 31 March 2010.
21. Schiavoni, M.; Campisi, S.; Carniti, P.; Gervasini, A.; Delplanche, T. Focus on the catalytic performances of Cu-functionalized hydroxyapatites in NH3-SCR reaction. *Appl. Catal. A* **2018**, *563*, 43–53. [CrossRef]
22. Galloni, M.G.; Campisi, S.; Marchetti, S.G.; Gervasini, A. Environmental Reactions of Air-Quality Protection on Eco-Friendly Iron-Based Catalysts. *Catalysts* **2020**, *10*, 1415. [CrossRef]